Turbo Demodulation of Zero-Padded OFDM Transmissions

Bertrand Muquet, *Member, IEEE*, Marc de Courville, *Member, IEEE*, Pierre Duhamel, *Fellow, IEEE*, Georgios B. Giannakis, *Fellow, IEEE*, and Pierre Magniez

***Abstract*—This letter extends turbo-demodulation to the zero-padded OFDM (ZP-OFDM) system by accounting for the noise color and the symbols estimates correlation introduced by equalization. Resorting to realistic simulations, we show that turbo-demodulation used with set partitioning labeling can significantly outperform noniterative decoding with Gray labeling. We also show that it increases the performance gap between ZP-OFDM and OFDM with cyclic prefix (CP-OFDM) relative to noniterative decoding, because it amplifies the performance gain due to the guaranteed symbol recovery of ZP-OFDM.**

***Index Terms*—HIPERLAN/2, IEEE802.11a, iterative demodulation, OFDM, zero-padding, ZP-OFDM.**

I. Introduction

In MODERN wireless systems, bit interleaving is preferred over symbol interleaving because it offers improved performance when communicating over Rayleigh channels [2]. The resulting bit-interleaved coded modulation (BICM) [2] includes channel coding, bit interleaving, and bit-to-complex-symbol mapping stages that are performed separately. With large-size constellations [(e.g., 16- or 64-quadrature amplitude modulation (QAM)], optimal BICM decoding is difficult because several encoded bits are assigned to the in-phase and quadrature components of the constellation, which makes maximum-likelihood (ML) decoding computationally prohibitive [3]. An iterative suboptimum decoder was proposed in [3] and [4] for frequency-flat channels in the presence of additive white noise (AWN).

On the other hand, it is well known that cyclic prefix (CP)-OFDM offers a simple way to convert frequency-selective finite impulse response (FIR) channels to flat faded subchannels. Thus, the aforementioned iterative decoder applies directly to CP-OFDM systems equipped with BICM [3]. Recently, it was proposed to replace the CP by zero-padding (ZP) [1]. Unlike CP-OFDM, the resulting ZP-OFDM transmitter guarantees symbol recovery regardless of the channel zero locations. The price to be paid is a slightly increased receiver complexity, since the fast Fourier transform (FFT)-based equalization of CP-OFDM is replaced by FIR filtering if minimum mean-square error (MMSE) equalization is performed at the receiver.

Up to now, only conventional noniterative decoding has been considered for ZP-OFDM. In this paper, we extend turbo-demodulation to ZP-OFDM. The challenge is that ZP-OFDM equalizers color the noise and introduce correlations between symbols estimates, so the BICM decoding has to be modified accordingly. Our simulations will rely on the constellation design rules of [4] to quantify the gain that can be obtained with turbo-demodulation of ZP-OFDM transmissions. They will also show that using ZP-OFDM rather than CP-OFDM at the transmitter allows for a reduction in the number of demodulation iterations. This may result in an overall smaller complexity of ZP-OFDM receivers (relative to CP-OFDM receivers), in spite of the more complex equalization needed for ZP-OFDM.

The rest of this paper is organized as follows. Section II reviews the iterative demodulation procedure, and Section III presents the ZP-OFDM transmitter and extends the iterative demodulation procedure to it. Section IV presents simulation results and conclusions.[1]

II. Turbo-Demodulation for BICM

The upper part of Fig. 1 depicts the discrete time-block diagram of a bit-interleaved modulator in the simple case of a rate $R = 1/2$ convolutional code and a 16–QAM modulation. The extension to other coding rates and other coherent modulations is straightforward. The modulator is composed of a convolutional encoder, an interleaver, and a bit-to-symbol mapper. Each block operates independently of the other ones. Each information bit b_i is first encoded into two bits, c_i^0 and c_i^1, which are interleaved in order to gain resilience against error bursts. The interleaved bits are then parsed in subsequences of four bits $d_k^1, \ldots, d_k^4$ which are mapped onto the complex symbols $s_k(d_k^1, \ldots, d_k^4)$ according to a given labeling map. Symbols s_k are then sent through the channel, which introduces frequency-flat Rayleigh fading with AWN. The received signal is then given by $y_k = h_k s_k(d_k^1, \ldots, d_k^4) + n_k$, where the channel coefficients h_k are independent and identically distributed (i.i.d.) random scalar complex gains drawn from a complex Gaussian distribution, and the noise samples n_k are scalar i.i.d. complex Gaussian with zero-mean and variance σ_n^2.

Paper approved by R. S. Cheng, the Editor for CDMA and Multiuser Communications Systems of the IEEE Communications Society. Manuscript received January 30, 2001; revised October 24, 2001. This paper was presented in part at the 34th Asilomar Conference on Signals and Systems, Pacific Grove, CA, October 29, 2000.

B. Muquet was with Motorola Labs, Paris, 91193 France. He is now with Stepmind, Boulogne-Billancourt, 92100 France (e-mail: bertrand.muquet@stepmind.com).

M. de Courville is with Motorola Labs, Paris, 91193 France (e-mail: Marc.de.Courville@crm.mot.com).

P. Duhamel is with CNRS/LSS, Supélec, Gif-Sur-Yvette, 91193 France (e-mail: pierre.duhamel@lss.supelec.fr).

G. B. Giannakis is with the University of Minnesota, Minneapolis MN 55455, USA (e-mail: georgios@ece.umn.edu).

P. Magniez was with the Ecole Nationale Supérieure des Télecommunications, Paris 75013, France.

Digital Object Identifier 10.1109/TCOMM.2002.805265

[1]We will use lower-case letters to denote bits or complex symbols. Lower-case boldface letters stand for sequences or vectors of either bits or symbols. Upper-case boldface letters are reserved for matrices.

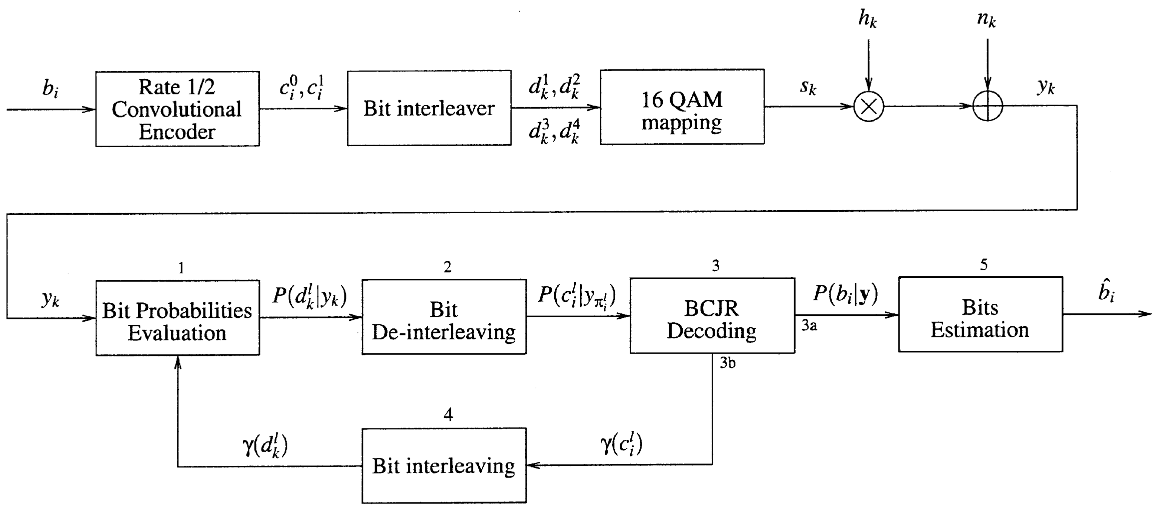

Fig. 1. BICM modulator and iterative demodulator.

Based on this transmission model, the receiver has to estimate the sequence of transmitted bits $\mathbf{b}$ from the sequence of received symbols $\mathbf{y}$, so as to minimize a given criterion [e.g., packet-error rate (PER)]. Toward this goal, $P(\mathbf{y}|\mathbf{b})$ has to be maximized. In practice, one works with the encoded bits since there is a one-to-one correspondence between information sequences and codewords. Thus, one looks for the ML-interleaved codeword $\hat{\mathbf{d}}$ in the set $\mathcal{D}$ of interleaved codewords given by

$$\hat{\mathbf{d}} = \arg\max_{\mathbf{d}\in\mathcal{D}} P(\mathbf{y}|\mathbf{d}) = \arg\max_{\mathbf{d}\in\mathcal{D}} \prod_k P\left(y_k | s_k(d_k^1, \ldots, d_k^4)\right) \tag{1}$$

where (??) comes from the fact that, traditionally, symbol estimates are assumed to be independent, and the noise is assumed to be white. In order to allow the bit deinterleaving to be performed, symbol probabilities are then approximated as $P\left(y_k|s_k(d_k^1,\ldots,d_k^4)\right) \approx \prod_{l=1}^4 P(d_k^l|y_k)$. The bit probabilities $P(d_k^l|y_k)$ can be computed using Baye's rule as

$$\begin{aligned} P(d_k^1|y_k) &= \sum_{d_k^2,d_k^3,d_k^4\in\{0,1\}} P(d_k^1,\ldots,d_k^4|y_k) \\ &= \sum_{d_k^2,d_k^3,d_k^4\in\{0,1\}} \frac{P(y_k|s(d_k^1,\ldots,d_k^4))P(d_k^1,\ldots,d_k^4)}{P(y_k)}. \end{aligned}$$

With large interleaver sizes, $P(d_k^1,\ldots,d_k^4) \approx P(d_k^1)\ldots P(d_k^4)$, which enables computation of the bit probabilities. Conventional noniterative procedures do not take into account the fact that bits d_k^l are encoded bits, and that some combinations of bits for various k and l combinations are prohibited by the encoder. In this case, no assumption is made on the *a priori* probabilities of the encoded bits which are assumed to take values 0 and 1 with the same probability. Thus, the bit probabilities are given by

$$P(d_k^1|y_k) \propto \sum_{d_k^2,\ldots,d_k^4\in\{0,1\}} \exp\left(-\frac{1}{2\sigma^2}\left|y_k - h_k s_k(d_k^1,\ldots,d_k^4)\right|^2\right)$$

from which an estimate of the information bits can be obtained by applying either the Viterbi or the Bahl–Cocke–Jelinek–Raviv (BCJR) algorithm [5].

The turbo-demodulation algorithm improves the bit-sequence estimation by iteratively accounting for the code structure in the inverse mapping process. With this goal, the *a posteriori* information obtained at the decoder output is used as *a priori* information on the encoded bits in the inverse sub-block mapping. The corresponding demodulation scheme [4] is depicted in the lower part of Fig. 1. It is detailed in a constructive manner in [3], and is only summarized below:

1. initialize the *a priori* information on the bits to be uniform;
2. perform the symbol-to-bit inverse mapping by taking into account the actual *a priori* information on the encoded bits (sub-block 1);
3. deinterleave the resulting bit probabilities to get the encoded bit probabilities $P(c_i^l|y_{\pi_i^l})$, where $y_{\pi_i^l}$ is the complex symbol carrying c_i^l. Then, feed $P(c_i^l|y_{\pi_i^l})$ to the decoding algorithm (sub-block 2);
4. use the BCJR decoding algorithm **[5]** to obtain the *a posteriori* probability (APP) of the information bits $P^{APP}(b_i|\mathbf{y})$ (output 3a of sub-block 3) and the extrinsic probabilities of the encoded bits, which are defined as $\gamma(c_i^l) \propto P^{APP}(c_i^l|\mathbf{y})/P(c_i^l|y_{\pi_i^l})$ (output 3b);
5. reinterleave the extrinsic probabilities in order to use them as *a priori* information $\gamma(d_k^l)$ in sub-block 1 (sub-block 4) to improve the inverse mapping;
6. iterate between Steps 2-5 as previously described;
7. after a given number of iterations, compute an estimate of the information bits $\hat{b}_i$ from the APPs $P^{APP}(b_i|\mathbf{y})$ (sub-block 5).

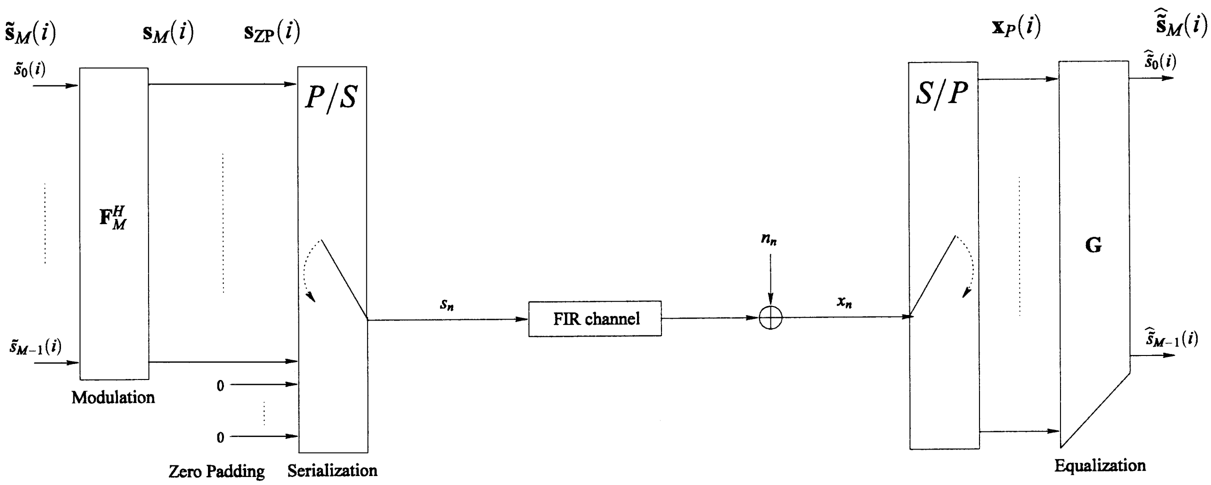

Fig. 2. Discrete model of a ZP-OFDM transceiver.

III. APPLICATION TO ZP-OFDM

It is well known that the channel effect on CP-OFDM amounts to a simple scalar multiplication of the symbol sent on each subcarrier by the corresponding channel attenuation and AWN. Thus, the previous method applies straightforwardly to CP-OFDM [3] and results in significant performance improvement if the interleaver and the constellation design rules of [4] are incorporated. Since symbol recovery is not guaranteed when some subcarriers are hit by channel nulls, it has been proposed in [1] to replace the CP by ZP, which ensures symbol recovery and leads to improved performance. In what follows, we extend turbo-demodulation to ZP-OFDM.

Fig. 2 depicts the baseband discrete-time model of ZP-OFDM. The $M \times 1$ digital input $\mathbf{s}_M(i)$ is first modulated by the IFFT matrix $\mathbf{F}_M^{\mathcal{H}}$ with entries $M^{-1/2}\exp\{j2\pi mk/M\}$. Then, L trailing zeros are padded at the end of the resulting vector $\tilde{\mathbf{s}}_M(i) = \mathbf{F}_M^{\mathcal{H}}\mathbf{s}_M(i)$. The corresponding $P \times 1$ transmitted vector $\mathbf{s}_{\text{ZP}}(i) = \mathbf{F}_{\text{ZP}}^{\mathcal{H}}\mathbf{s}_M(i)$, where $\mathbf{F}_{\text{ZP}}^{\mathcal{H}} = [\mathbf{F}_M\mathbf{0}]^{\mathcal{H}}$ is then serialized and transmitted through the Lth-order FIR channel with impulse response h_l, where $h_l = 0$, $\forall l \notin [0, L]$. The all-zero $M \times L$ submatrix $\mathbf{0}$ in $\mathbf{F}_{\text{ZP}}^{\mathcal{H}}$ eliminates interblock interference. Let $\mathbf{H} = [\mathbf{H}_0, \mathbf{H}_{\text{ZP}}]$ denote a partition of the $P \times P$ convolution matrix $(\mathbf{H})_{ij} = h_{i-j}$ with $\mathbf{H}_0$ and $\mathbf{H}_{\text{ZP}}$ constituting its first M and last L columns, respectively. The received $P \times 1$ vector is then $\mathbf{x}_P(i) = \mathbf{H}\mathbf{F}_{\text{ZP}}^{\mathcal{H}}\mathbf{s}_M(i) + \mathbf{n}_P(i) = \mathbf{H}_0\mathbf{F}_M^{\mathcal{H}}\mathbf{s}_M(i) + \mathbf{n}_P(i)$, where $\mathbf{n}_P(i)$ represents the noise samples. The $P \times M$ matrix $\mathbf{H}_0$ is Toeplitz and is always guaranteed to be invertible, which enables symbol recovery regardless of the channel zero locations, unlike CP-OFDM.

In what follows, only MMSE equalization is considered, but it is possible to extend the procedure to other equalizers. For white noise with variance σ_n^2, the MMSE equalizer is given by [1] $\mathbf{G} = \mathbf{R}_{\mathbf{ss}}\mathbf{F}_M\mathbf{H}_0^{\mathcal{H}}(\sigma_n^2\mathbf{I}_P + \mathbf{H}_0\mathbf{F}_M^{\mathcal{H}}\mathbf{R}_{\mathbf{ss}}\mathbf{F}_M\mathbf{H}_0^{\mathcal{H}})^{-1}$, where $\mathbf{R}_{\mathbf{ss}}$ stands for the signal autocorrelation matrix. From $\mathbf{x}_P$ (we drop the index i for brevity), an estimate of $\tilde{\mathbf{s}}_M$ is given by

$$\hat{\mathbf{s}}_M = \mathbf{G}\mathbf{x}_P = \mathbf{G}\mathbf{H}_0\mathbf{F}_M^H\mathbf{s}_M + \mathbf{G}\mathbf{n}_P.$$

Let us define $\boldsymbol{\Delta} = \mathbf{G}\mathbf{H}_0\mathbf{F}_M^H$ and let $\mathbf{D}$ be the diagonal matrix whose main diagonal is equal to that of $\boldsymbol{\Delta}$ and $\boldsymbol{\Delta}_d = \boldsymbol{\Delta} - \mathbf{D}$. The latter term can be decomposed as a sum of three terms: $\hat{\mathbf{s}}_M = \mathbf{D}\mathbf{s}_M + \boldsymbol{\Delta}_d\mathbf{s}_M + \mathbf{G}\mathbf{n}_P$. Hence, both the independence between symbol estimates and the AWN assumptions used in (1) no longer hold. We propose in this letter to take into account the noise coloration (multiplication of $\mathbf{n}_P$ by $\mathbf{G}$), the bias that can be introduced by the equalizer (represented by matrix $\mathbf{D}$), and the error introduced by the symbol estimates crosscorrelation $\boldsymbol{\Delta}_d\tilde{\mathbf{s}}_M$.

The first thing we do is to unbias the equalizer in order to avoid a decision mismatch, which would result in degraded performance (note that the bias could also be accounted for directly in the metrics). Let us define $\hat{\mathbf{s}}_M^{\text{ub}}$ as $\hat{\mathbf{s}}_M^{\text{ub}} = \mathbf{D}^{-1}\hat{\mathbf{s}}_M = \mathbf{s}_M + \mathbf{D}^{-1}\boldsymbol{\Delta}_d\mathbf{s}_M + \mathbf{D}^{-1}\mathbf{G}\mathbf{n}_P$. At this point, the symbol estimates crosscorrelation and the thermal noise can be gathered into a single noise term $\mathbf{n}_{\mathbf{G}} = \mathbf{D}^{-1}\left[\boldsymbol{\Delta}_d\tilde{\mathbf{s}}_M + \mathbf{G}\mathbf{n}_P\right]$, and the problem with ZP-OFDM is that the noise term $\mathbf{n}_{\mathbf{G}}$ is not white and has covariance matrix

$$\mathbf{R}_{\mathbf{n}_{\mathbf{G}}\mathbf{n}_{\mathbf{G}}} = \mathbf{D}^{-1}\left[\boldsymbol{\Delta}_d\mathbf{R}_{\mathbf{ss}}\boldsymbol{\Delta}_d^H + \mathbf{G}\mathbf{R}_{\mathbf{nn}}\mathbf{G}^H\right]\mathbf{D}^{-H}.$$

In order to form trellis metrics for ZP-OFDM, the log-likelihood symbol metric has to be considered

$$\log P(\mathbf{x}_P|\mathbf{s}_M) = \left[\hat{\mathbf{s}}_M^{\text{ub}} - \mathbf{s}_M\right]^H \mathbf{R}_{\mathbf{n}_{\mathbf{G}}\mathbf{n}_{\mathbf{G}}}^{-1}\left[\hat{\mathbf{s}}_M^{\text{ub}} - \mathbf{s}_M\right]. \quad (2)$$

Hence, factoring out the probabilities to simplify the ML optimization in (2) is not as simple as in traditional OFDM systems with CP [see (1)].

We propose to approximate the noise samples of $\mathbf{n}_{\mathbf{G}}$ as being independent but not identically distributed, and to approximate the covariance matrix of $\mathbf{n}_{\mathbf{G}}$ by its main diagonal

$$\mathbf{R}_{\mathbf{n}_{\mathbf{G}}\mathbf{n}_{\mathbf{G}}} \approx \text{Diag}\left(\mathbf{D}^{-1}\left[\boldsymbol{\Delta}_d\mathbf{R}_{\mathbf{ss}}\boldsymbol{\Delta}_d^H + \mathbf{G}\mathbf{R}_{\mathbf{nn}}\mathbf{G}^H\right]\mathbf{D}^{-H}\right).$$

This approximation is valid when a large-size interleaver is used, and is the one classically made in literature when dealing with colored noise. That way, (2) becomes

$$\log P(\mathbf{x}_P|\mathbf{s}_M) \approx \sum_{k=1}^{M}\left[\mathbf{R}_{\mathbf{n}_{\mathbf{G}}\mathbf{n}_{\mathbf{G}}}^{-1}\right]_{k,k}\left|\hat{s}_k^{\text{ub}} - s_k\right|^2$$

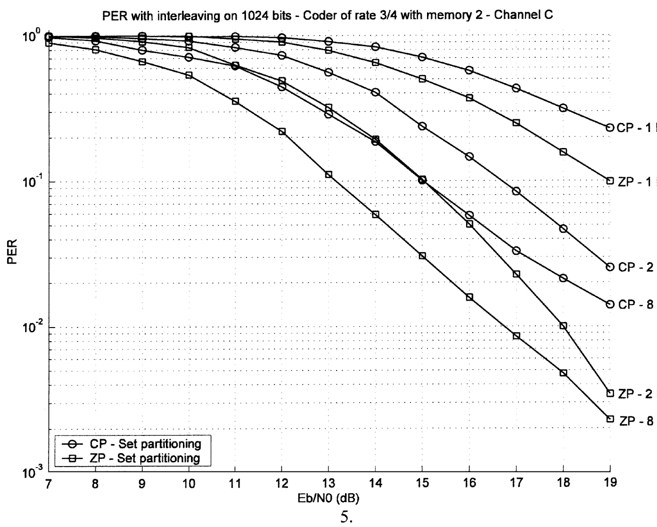

Fig. 3. CP- and ZP-OFDM with iterative decoding.

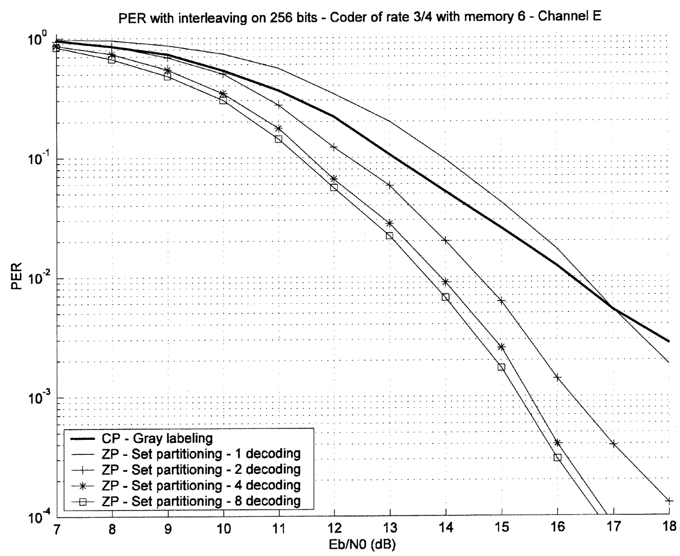

Fig. 4. Potential gain for Hiperlan/2.

and the same simplified trellis decoding as for CP-OFDM can be performed with only a small extra complexity added for computing the diagonal entries of $\mathbf{R}_{\mathbf{n_G n_G}}^{-1}$. The latter, though, is channel dependent and has to be updated each time the channel varies.

Note that ML decoding in the presence of colored noise is a nontrivial problem (see, e.g., [6]). Besides, the approximation we have done is already required in order to perform trellis decoding with bit interleaving, and hence, it can be thought that it will not seriously affect the decoder performance. However, it may lead to problems, especially with small interleaver sizes, and we resort to simulations to verify that the approximation is reasonable.

IV. Simulations and Conclusions

Simulations have been conducted with the parameters of the new European standard for wireless local area network Hiperlan/2 (HL2), that is, with $M = 64$ carriers and $L = 16$ CP or ZP samples. They have been obtained by running Monte Carlo realizations with each trial corresponding to a different realization of the channel models C (typical office environment) and E (large delay spread office environment) described in [7]. During a frame, the channel is time invariant and is exactly known at the receiver.

Fig. 3 depicts PER for channel C. Results are given for a 16–QAM constellation with set partitioning (SP) labeling for a random interleaver of size 1024, and a rate $R = 3/4$ convolutional encoder defined in octal form by (5,7). It can be observed that the signal-to-noise ratio required to obtain a PER of 10^{-2} is reduced by more than 2 dB if ZP-OFDM is used instead of CP-OFDM. Note that the performance of ZP-OFDM after two decoding steps is better than that of CP-OFDM after eight iterations. Hence, equalization complexity is not the only point to consider if iterative decoding is used. It can also be inferred that the performance gap between CP and ZP is enlarged with iterative decoding (it is enlarged from 1 to 2 dB after iterations). Intuitively, it is probably because the improved equalization capabilities allow the ZP to provide a better feedback, which then results to a better demapping compared to CP, and so forth and so on.

Fig. 4 illustrates for channel E the performance gain that could be obtained in HL2 if SP and ZP-OFDM were employed. HL2 specifies a CP-OFDM transmitter with Gray labeling for the modulation, which result in a small performance gain with iterative decoding [3]. Note that the encoder and the interleaver size used for this simulation are those of HL2: the interleaver operates on 256 bits and the encoder is obtained from the rate 1/2 encoder efined in octal form by (133 171) by puncturing it to rate 3/4. Note that a random interleaver has been used for ZP-OFDM with SP because the currently standardized one is not appropriate for iterative decoding. Note that with the proposed changes (ZP, labeling, interleaving), though not having an impact on the transmitter complexity, the decoding delay and the data rate allow gains of about 3.5 dB to obtain $PER = 10^{-2}$ compared to the solution currently standardized. This shows that ZP-OFDM and iterative decoding can be successfully applied in real applications, and should be considered in the future for robust transmissions.

References

[1] A. Scaglione, G. B. Giannakis, and S. Barbarossa, "Redundant filterbank precoders and equalizers – Part I : Unification and optimal designs, and Part II : Blind channel estimation, synchronization and direct equalization," *IEEE Trans. Signal Processing*, vol. 47, pp. 1988–2022, July 1999.

[2] G. Caire, G. Taricco, and E. Biglieri, "Bit-interleaved coded modulation," *IEEE Trans. Inform. Theory*, vol. 44, pp. 927–946, May 1998.

[3] P. Magniez, B. Muquet, P. Duhamel, V. Buzenac, and M. de Courville, "Optimal decoding of bit-interleaved modulations: Theoretical aspects and practical algorithms," in *Proc. Int. Symp. Turbo Codes and Related Topics*, Brest, France, Sept. 2000, pp. 169–172.

[4] X. Li and J. A. Ritcey, "Trellis-coded modulation with bit interleaving and iterative decoding," *IEEE J. Select. Areas Commun.*, vol. 17, pp. 715–724, Apr. 1999.

[5] L. Bahl, J. Cocke, F. Jelinek, and J. Raviv, "Optimal decoding of linear codes for minimizing symbol error rate," *IEEE Trans. Inform. Theory*, pp. 284–287, Mar. 1974.

[6] S. A. Alketar and J. K. Wolf, "Improvements in detectors based upon colored noise," *IEEE Trans. Magn.*, vol. 34, pp. 94–97, Jan. 1998.

[7] "Channel models for HIPERLAN/2 in different indoor scenarios," European Telecommun. Standards Inst., ETSI Normalization Commitee, Sophia-Antipolis, Valbonne, France, Norme ETSI, 1998.